Supporting Information

On the interfacial lithium dynamics in $Li_7La_3Zr_2O_{12}$:poly(ethylene oxide)(LiTFSI) composite polymer-ceramic solid electrolytes under strong polymer phase confinement

Mauricio R. Bonilla[1], Fabián A. García Daza[2], Henry A. Cortés[1], Javier Carrasco[3], and Elena Akhmatskaya[1,4]

[1]Basque Center for Applied Mathematics, Alameda de Mazarredo 14 (48009) Bilbao, Spain
[2]Department of Chemical Engineering and Analytical Science, The University of Manchester, Manchester M13 9PL, United Kingdom
[3]Centre for Cooperative Research on Alternative Energies (CIC energiGUNE), Basque Research and Technology Alliance (BRTA), Alava Technology Park, Albert Einstein 48, 01510, Vitoria-Gasteiz, Spain
[4]IKERBASQUE, Basque Foundation for Science, Plaza Euskadi 5 (48009), Spain

Table S1: Point charges in the PEO(LiTFSI) ststem

Species	Location	Charge
O_1	-O-H termination in PEO	0.683
O_2	-CH_2-O-CH_2- in PEO	-0.400
H_1	-O-H termination in PEO	0.418
H_2	-CH_2-OH in PEO	0.060
H_3	-CH_2-O-CH_2- in PEO	0.030
C_1	-CH_2-OH in PEO	0.145
C_2	-CH_2-O-CH_2- in PEO	0.140
Li	LiTFSI	0.70
F	LiTFSI	-0.16
C_3	LiTFSI	0.35
S	LiTFSI	1.02
O_3	LiTFSI	-0.53
N	LiTFSI	-0.36

S1. Validation of the force field for the PEO(LiTFSI) system

To validate the coupling of the PEO [1] and LiTFSI [2] force fields, the bulk conductivities of PEO(LiTFSI) reported by the experimental work of Lascaud et al. [3] and those calculated in this work, are depicted in Fig. S1 for two different temperatures and a wide range of EO:Li ratios. The point charges are summarized in Table S1.

S2. Density profiles for Li_g^+

The distribution of Li_g^+ appears to differ significantly between the panels of Figure 2. However, this effect arises due to the different scales of the x-axis. Figure S2 depicts Li_g^+ for $\Delta = 1, 2.5$ and 5 nm, but removing the gap confining the polymer phase and putting all of the curves within the same scale. By doing this, it becomes evident that the differences are relatively minor. The reasons for such differences are discussed in Section 3 of the manuscript.

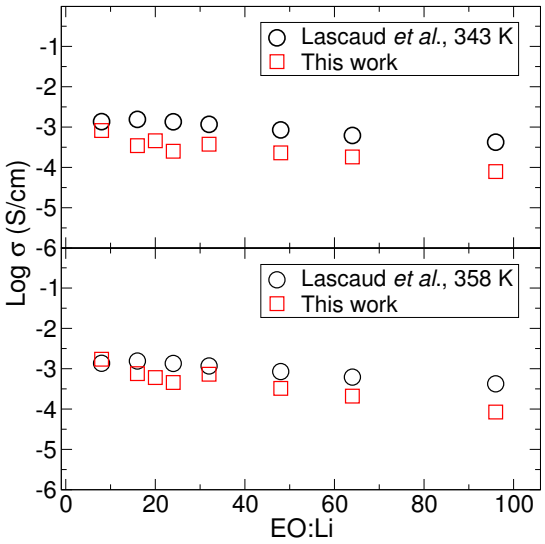

Figure S1: Computed (this work) and experimental [4] ionic conductivity in PEO(LiTFSI) as a function of EO:Li ratio at 343 K and 358 K. Reprinted with permission from ref. [3]. Copyright 2021 American Chemical Society.

S3. Relationship between gap and volume fraction

If the filler particles are uniformly distributed in the CSSE, then the average interparticle distance is related to the average particle diameter, d_p, and the number of filler particles per unit volume, C, through

$$\Delta \sim d_p + C^{-1/3}, \tag{1}$$

C can be expressed in terms of volume fraction ω through $C = \frac{6\omega}{\pi d_p^3}$. Substituting into eq. (1) and solving for ω yields

$$\omega \sim \frac{\pi}{6}(\Delta/d_p + 1)^{-3}. \tag{2}$$

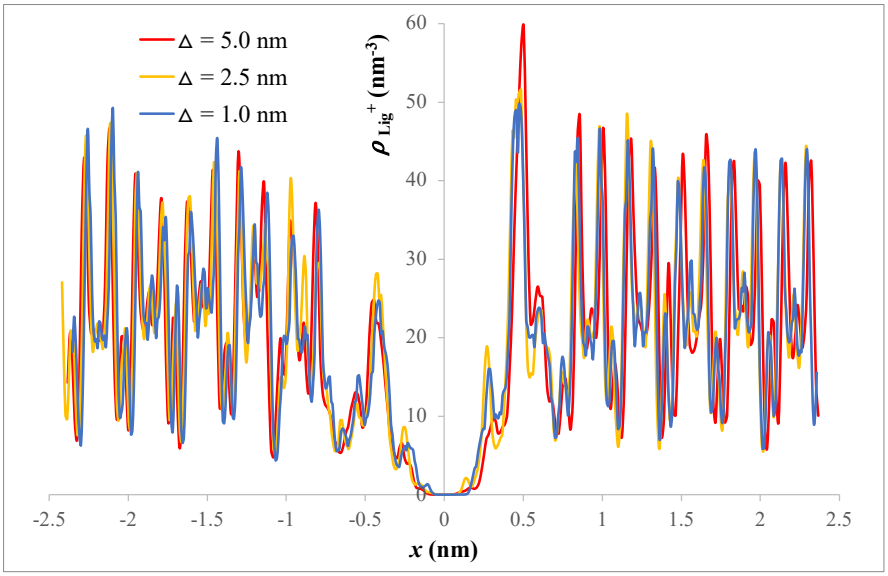

Figure S2: Density profiles for Li_g^+ in the structures with $\Delta = 1, 2.5$ and 5 nm, removing the polymer phase.

S4. Density profiles for $1 < \Delta < 5$ nm and $N = 20$

Figure S3 depicts the number density profiles (atoms per nm^3), ρ_i, for selected atoms in the CSSE, for $1 < \Delta < 5$ nm and $N = 20$, where N is the number of EO units in the polymer (Figures for $N = 10$ are essentially identical, and are found in the manuscript).

S5. The importance of considering local differences in the density profiles

Figure S4 shows the density profiles of Li_p^+ (lithium originating in the polymer), C and O_p (oxygen originating in the polymer), at 450 K and for $N = 20$. While the solid blue and green lines represents C and O_p atoms from bound PEO chains, respectively, the dotted lines represents C and O_p atoms from all PEO chains. When the entire volume of the simulation box is used (such as in Figure S4), the relationship between the Li_p^+ profile and the C and O_p profiles is unclear. The dashed vertical lines designate the lowest and highest x values at which corresponding solid and dotted lines converge. There is no obvious relationship between such values and the points at which the Li_p^+

profile vanishes as it approaches the interface. Similarly, the dot-dashed vertical lines represent the lowest and highest x values at which corresponding solid and dotted lines differ by less than 1 %. Again, no obvious relationship is detected between these values and the behavior of the Li_p^+ profile. If instead of the entire simulation box, smaller slices are taken (such as in Figure 6 of the manuscript), a relationship becomes transparent.

S6. Transport parallel to the interface

In order to investigate Li-ion diffusion parallel to the garnet surface in the polymer phase, we follow the formulation by Liu et al. [J. Phys. Chem. B (2004), 108, 6595-6602], briefly summarized below.

Let $N_{\{x_1,x_2\}}(t, t+\tau)$ be the number of particles that stay within the region $\{x_1, x_2\}$ for $(t, t+\tau)$ period of time. The mean square displacement in the y direction inside $\{x_1, x_2\}$ is defined as

$$\langle y(\tau)^2 \rangle_{\{x_1,x_2\}} = \frac{1}{n_t} \sum_{t=1}^{n_t} \frac{1}{N_{\{x_1,x_2\}}(t,t)} \sum_{i \in N_{\{x_1,x_2\}}(t,t+\tau)} (y_i(t,t+\tau) - y_i(t))^2, \quad (3)$$

where n_t is the total number of time steps averaged over. The survival rate $R(\tau)$, representing the average fraction of particles remaining for a period of at least τ within $\{x_1, x_2\}$ is

$$R(\tau) = \frac{1}{n_t} \sum_{t=1}^{n_t} \frac{N_{\{x_1,x_2\}}(t,t+\tau)}{N_{\{x_1,x_2\}}(t,t)}. \quad (4)$$

With the definitions above, the diffusion coefficient in y can be estimated from

$$D_{yy}(\{x_1, x_2\}) = \lim_{\tau \to +\infty} \frac{\langle y(\tau)^2 \rangle_{\{x_1,x_2\}}}{2\tau R(\tau)}, \quad (5)$$

and analogously for $D_{zz}(\{x_1, x_2\})$. The diffusion coefficient parallel to the interface is then calculated as

$$D = \frac{1}{2}(D_{yy} + D_{zz}). \quad (6)$$

S7. Umbrella sampling calculations

We pre-selected a distance between consecutive US windows of 0.05 nm, which we considered a suitable resolution to track the energy cost of a lithium

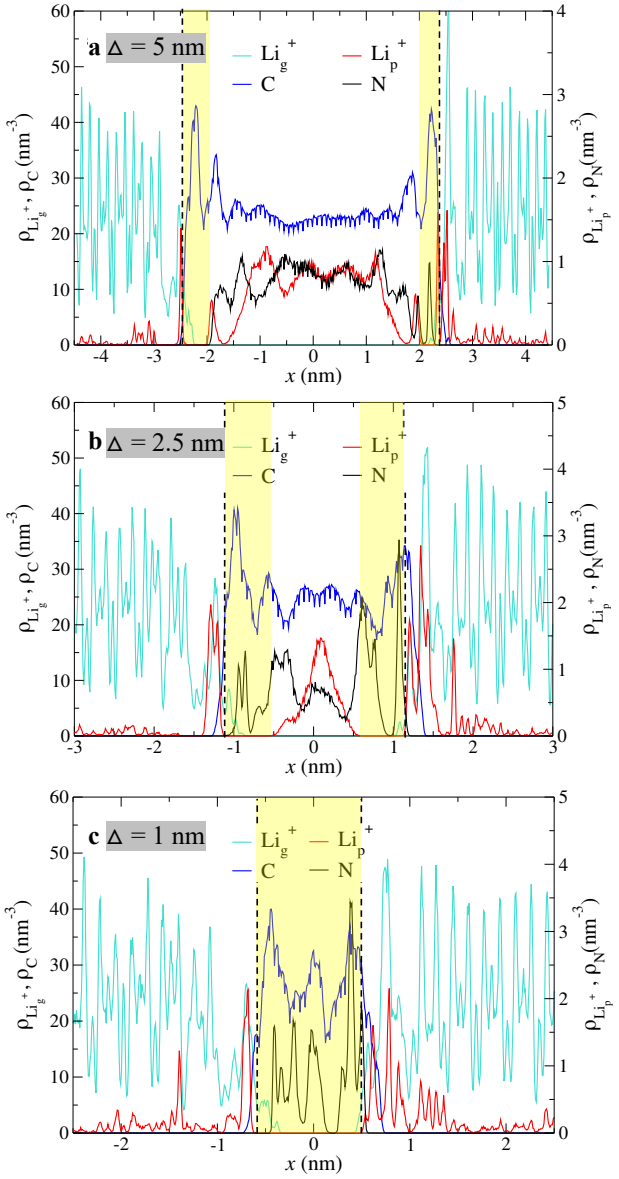

Figure S3: Density profiles for selected atoms in the CSSE at 450 K and for $N = 20$: C atoms from PEO (blue), N atoms from the $TFSI^-$ anions (black), Li^+ ions *originating* in the garnet phase, Li_g^+ (cyan), and the polymer phase, Li_p^+ (red). The profiles correspond to three different gaps: **a** $\Delta = 5$ nm, **b** $\Delta = 2.5$ nm, and **c** $\Delta = 1.0$ nm. The yellow bands represent Li^+ free layers on the polymer side of the interface. The dashed lines indicate the limits of the garnet surfaces.

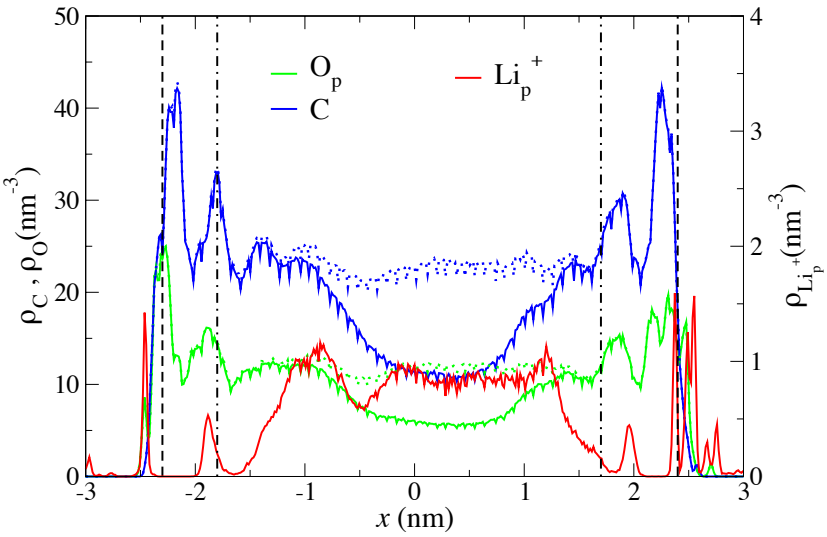

Figure S4: Density profiles $\rho_X(x)$ for X =Li_p^+, C and O_p, at 450 K and for $N = 20$. The solid blue (green) line represents C (O_p) atoms from bound PEO chains, while the dotted blue (green) line represents C (O_p) atoms from all chains. The dashed vertical lines designate the lowest and highest x values at which corresponding solid and dotted lines merge. Conversely, the dot-dashed vertical lines represent the lowest and highest x values at which corresponding solid and dotted lines differ by less than 1 %.

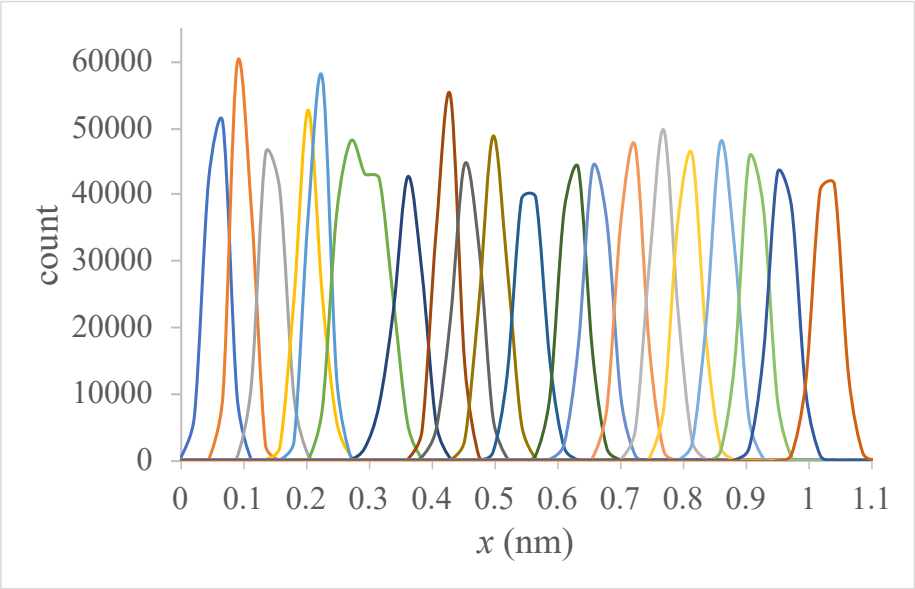

Figure S5: Weighted histogram analysis method for the umbrella sampling calculations in site 1, using a window separation of 0.05 nm, $K = 5000$ kJ mol^{-1}nm^{-2} and 5 ns MD runs per window.

extraction. Subsequently, we tested three spring constants K: 5000, 10000 and 50000 kJ mol^{-1}nm^{-2} on the Li^+ ion on site 1 (Figure 3a) based on 5 ns NVT MD runs at 450 K. The results where then interpreted using the weighted histogram analysis method. Our criterion to select a particular K ensured that (i) the peak of each histogram was effectively located around the window center, and (ii) contiguous histograms overlapped. If K is too small, the histogram peak is displaced towards the direction of decreasing free energy. If K is too large, inadequate overlapping is obtained. We found that both conditions (i) and (ii) were satisfied by taking $K = 5000$ kJ mol^{-1}nm^{-2} (see Figure S5).

References

[1] W. L. Jorgensen, D. S. Maxwell, and J. Tirado-Rives, "Development and testing of the opls all-atom force field on conformational energetics and properties of organic liquids," *Journal of the American Chemical Society*, vol. 118, no. 45, pp. 11225–11236, 1996.

[2] T. Köddermann, D. Paschek, and R. Ludwig, "Molecular dynamic simula-

tions of ionic liquids: A reliable description of structure, thermodynamics and dynamics," *ChemPhysChem*, vol. 8, no. 17, pp. 2464–2470, 2007.

[3] S. Lascaud, M. Perrier, A. Vallee, S. Besner, J. Prud'homme, and M. Armand, "Phase Diagrams and Conductivity Behavior of Poly(ethylene oxide)-Molten Salt Rubbery Electrolytes," *Macromolecules*, vol. 27, no. 25, pp. 7469–7477, 1994.

[4] M. R. Bonilla, F. A. García Daza, P. Ranque, F. Aguesse, J. Carrasco, and E. Akhmatskaya, "Unveiling interfacial li-ion dynamics in li7la3zr2o12/peo(litfsi) composite polymer-ceramic solid electrolytes for all-solid-state lithium batteries," *ACS Applied Materials & Interfaces*, vol. 13, pp. 30653–30667, 07 2021.